Free Radical Biology and Medicine 168 (2021) 234–246

Contents lists available at ScienceDirect

Free Radical Biology and Medicine

journal homepage: www.elsevier.com/locate/freeradbiomed

Original article

Ginkgolide B monotherapy reverses osteoporosis by regulating oxidative stress-mediated bone homeostasis

Chien-Wei Lee [a,b,c], Hui-Chu Lin [a], Belle Yu-Hsuan Wang [c], Amanda Yu-Fan Wang [c], Rita Lih-Ying Shin [c], Stella Yee Lo Cheung [c], Oscar Kuang-Sheng Lee [a,c,d,e,*]

[a] Institute for Tissue Engineering and Regenerative Medicine, The Chinese University of Hong Kong, Hong Kong SAR, 999077, China
[b] School of Biomedical Sciences, Faculty of Medicine, The Chinese University of Hong Kong, Hong Kong SAR, 999077, China
[c] Department of Orthopedics and Traumatology, Faculty of Medicine, Prince of Wales Hospital, The Chinese University of Hong Kong, Hong Kong SAR, 999077, China
[d] Li Ka Shing Institute of Health Sciences, The Chinese University of Hong Kong, Prince of Wales Hospital, Shatin, Hong Kong SAR, 999077, China
[e] Department of Orthopedics, China Medical University Hospital, Taichung, Taiwan

ARTICLE INFO

Keywords:
Ginkgo biloba extract
Osteoporosis
ROS
Ginkgolide B
Aging
Glucocorticoids

ABSTRACT

Osteoporosis is characterized by reductions in bone mass, which could be attributed to the dysregulation of bone homeostasis, such as the loss of balance between bone-resorbing osteoclasts and bone-forming osteoblasts. Elevated levels of oxidative stress increase bone resorption by promoting osteoclastogenesis and inhibiting the osteogenesis. Ginkgolide B (GB), a small natural molecule from *Ginkgo biloba*, has been reported to possess pharmacological activities by regulating reactive oxygen species (ROS) in aging-related degenerative diseases. Herein, we assessed the therapeutic effects of GB on the bone phenotypes of mice with osteoporosis induced by (I) aging, (II) ovariectomy, and (III) glucocorticoids. In all three animal models, oral gavage of GB significantly improved bone mass consistent with the increase in the OPG-to-RANKL ratio. In the in vitro experiments, GB promoted osteogenesis in aged mesenchymal stem cells (MSCs) and repressed osteoclastogenesis in aged macrophages by reducing ROS. The serum protein profile in GB-treated aged mice revealed moderate rejuvenating effects; signaling pathways associated with ROS were also regulated. The anabolic and anti-catabolic effects of GB were illustrated by the reduction in ROS. Our results indicate that GB is effective in treating osteoporosis. The use of GB in patients with osteoporosis is worthy of further clinical investigation.

1. Introduction

Lifespan extension is an excellent achievement owing to the improvements in medicine and public health worldwide; however, it is accompanied by an increased incidence of aging-related diseases, especially osteoporosis. Osteoporosis and related fractures are among the leading contributors to aging-related socioeconomic burdens in high-income and low-income countries [1]. The absolute number of age-related hip fractures is progressively increasing because of the increase in the aged population [2,3]. Thirty-three percent of women and twenty percent of men over the age of 50 will experience an osteoporosis-associated fracture. From 2020 to 2025, osteoporosis and associated fractures will likely be responsible for approximately 25.3 billion USD in costs in the US annually. Such a burden is forecasted to increase continuously due to the rapidly growing aged population.

Osteoporosis is characterized by low bone density and bone quality and compromised bone strength. Although the etiology of bone loss varies, these factors are associated with bone homeostasis. Bone homeostasis is controlled by the bone remodeling cycle, including consecutive bone resorption and bone formation, which is coordinated by bone-resorbing osteoclasts derived from macrophages and bone-forming osteoblasts derived MSCs. The coupling of bone resorption and bone formation is critical for securing bone replenishment and involves osteogenic factors released by osteoblasts. A shift in the balance

Abbreviations: BMD, bone mineral density; DEP, differentially expressed protein; GB, ginkgolide B; GBE, *Ginkgo biloba* extract; MPD, multiple population doubling; MSC, mesenchymal stem cell; Mϕ, macrophage; OB, MSC-derived osteoblast; OC, macrophage-derived osteoclast; OVX, ovariectomy; ROS, reactive oxygen species.

* Corresponding author. Department of Orthopedics, China Medical University Hospital, Taichung, Taiwan.
E-mail addresses: chienweilee@cuhk.edu.hk, icehikki@gmail.com (C.-W. Lee), zeoylintw@gmail.com (H.-C. Lin), bellewang@link.cuhk.edu.hk (B.Y.-H. Wang), yufan.wang@link.cuhk.edu.hk (A.Y.-F. Wang), 1155116078@link.cuhk.edu.hk (R.L.-Y. Shin), stellayl@link.cuhk.edu.hk (S.Y.L. Cheung), oscarlee9203@gmail.com (O.K.-S. Lee).

https://doi.org/10.1016/j.freeradbiomed.2021.03.008
Received 4 January 2021; Received in revised form 24 February 2021; Accepted 7 March 2021
Available online 27 March 2021

toward bone resorption that is observed in aging and other pathological conditions is collectively associated with the loss of bone mass and microarchitecture deterioration [4–7].

ROS have been demonstrated to regulate bone homeostasis during physiological steady-state conditions, aging and various pathological conditions. Increasing evidence indicates tight regulation of osteoporosis by ROS, such as hydrogen peroxide and superoxide [8,9]. During aging, excessive ROS in bone is attributed to the downregulation of ROS scavengers, such as Sod and catalase [10,11]. ROS impair the osteogenic potential of MSCs by inhibiting the canonical Wnt/β-catenin signaling pathway, which is indispensable for osteogenesis [12]; moreover, ROS also promote osteoclastogenic differentiation, together with aging-related osteoporosis [11]. In addition, ROS also regulate osteoblast-osteoclast communication, particularly through the osteoprotegerin-receptor activator of nuclear factor kappa-B-receptor activator of nuclear factor kappa-B ligand (OPG-RANK-RANKL) system. RANKL, which is stimulated and released by intracellular ROS levels in aged MSCs and osteoblasts, interacts with and activates RANK on the surface of macrophages to induce osteoclastogenesis, and this interaction is prevented by the decoy receptor OPG [13,14]. Although many new medicines have been developed that mainly focus on either preventing osteoclastic bone resorption or promoting bone formation, the efficacies of these treatments are relatively minor [15]. Moreover, long-term use of anti-resorptive drugs, such as bisphosphonates, increases skeletal fragility and osteonecrosis of the jaw due to disrupted coupling of bone resorption and formation [16,17]. Therefore, it is urgent to develop a new treatment that could reverse the imbalance in bone homeostasis by simultaneously promoting osteogenesis and reducing osteoclastogenesis.

Recently, small natural molecules have been considered promising medicinal products for treating aging-related diseases [18]. Among these potential candidates, ginkgolide B (GB), a unique component of *Ginkgo biloba* extract [19], exerts therapeutic efficacy in many aging-related degenerative conditions, including Parkinson's disease, Alzheimer's disease, and cerebrocardiovascular diseases [20], by inhibiting ROS and inflammation [21,22]. A previous study showed that intraperitoneal injection of GB exerts therapeutic effects on ovariectomy (OVX)-induced osteoporosis by activating osteoblast differentiation [23]. Given that aging-related osteoporosis is a complex and heterogeneous disease with different etiologies than OVX-induced osteoporosis [24], there remains a knowledge gap regarding the efficacy of GB in aging-related osteoporosis and the mechanism of action.

In this study, we elucidated the therapeutic efficacy of orally administered GB in osteoporosis and during steady-state conditions. We demonstrated that GB improved bone mass and microarchitecture in mouse models of osteoporosis (aging-, OVX- and glucocorticoid-induced osteoporosis) and under steady-state conditions. This bone-protective effect of GB was based not only on direct promotion of osteoblast mineralization but also on the repression of bone-degrading osteoclasts. GB reduced the expression levels of ROS, as indicated by the circulating proteomic profile and aged bone cells, to rebalance bone homeostasis. Our findings demonstrated that GB monotherapy restored bone remodeling in various animal models. Since pharmacological studies revealed that multiple-dose administration of GB in young healthy human subjects was well tolerated and exhibited an acceptable safety profile [25,26], GB supplementation may be a promising translational opportunity for preventing and treating osteoporosis.

2. Materials and methods

2.1. Chemicals

Ginkgolide B (#G6910), ginkgolide C (#18309), (−)-bilobalide (#B9031) and Ginkgo biloba extract (GBE) (#NIST3247) were purchased from Sigma-Aldrich (Sigma-Aldrich, St. Louis, MO, USA). Ginkgolide J (#ASB-00007186-010) was purchased from ChromaDex (ChromaDex, Irvine, CA, USA).

2.2. Animal models

For the aging models, 3- and 20-month-old female C57BL/6 mice were administered GB (12 mg/kg body weight) for two months. For the steady-state condition model, 6-month-old female C57BL/6 mice were administered GB (12 mg/kg body weight) for two months. For the ovariectomy (OVX) mouse model, 6-week-old C57BL/6 female mice underwent ovariectomy or sham operation. At three weeks after ovariectomy, OVX mice received a daily oral gavage of GB (3 and 12 mg/kg body weight) for two months. For glucocorticoid-induced osteoporosis, female C57BL/6 mice (10 weeks old) were intraperitoneally injected with dexamethasone (Dex) (#D4902, Sigma-Aldrich) (20 mg/kg body weight) daily to induce bone loss, and then the Dex-injected mice were subjected to Dex and Dex + GB treatment for an additional 14 days. GB was diluted to the appropriate concentration in 100 μL of PBS (#10378016, Gibco) for daily oral gavage. Mice were obtained from Laboratory Animal Services Centre, the Chinese University of Hong Kong and randomly assigned to control and experimental groups in all experiments. Animal experiments were conducted in a blinded manner where possible. We assured that all animals received humane care according to the criteria outlined in the "Guide for the Care and Use of Laboratory Animals" prepared by the National Academy of Sciences and published by the National Institutes of Health (NIH publication 86–23, revised 1985).

2.3. Blood biochemical analyses

Serum was collected by cardiac puncture to perform biochemical analysis. Briefly, serum was placed on SPOTCHEM test strips and measured by using a SPOTCHEM™ dry-chemistry clinical analyzer (ARKRAY Inc. Kyoto, Japan).

2.4. Skeletal phenotyping

BMD and the trabecular bone morphological parameters of isolated femurs were analyzed by microcomputed tomography (MILabs, U-CT, Heidelberglaan, The Netherlands) as previously described [27]. Briefly, the isolated femurs were fixed in formaldehyde overnight. The scanning was performed at a maximum tube voltage of 50 kVp, a current of 0.48 mA, an integration time of 200 m s, and a resolution of 20 μm. The scanning angular rotation was 360° with an angular step of 0.25°. Bone reconstruction of the femur was performed using 3DimViewer software and SCANCO Medical microCT software.

2.5. Quantitative proteomics analysis

Quantitative proteomics analysis was performed as previously described [28]. Briefly, the extracted peptides from serum samples were analyzed by LTQ-Orbitrap hybrid tandem mass spectrometry (Thermo Fisher Scientific, Waltham, MA, USA). Protein identification and quantification were performed by using PEAKS software. The DEP list was obtained using a 1.5-fold cutoff, a false discovery rate <1%, and a significance threshold of $p < 0.05$. The PANTHER classification system (www.pantherdb.org) was applied to the DEPs for Gene Ontology annotation. Heat maps were created of the collected protein expression levels through the data visualization tool BioVinci (version 1.1.5, vinci.bioturing.com).

2.6. Cell culture

Mouse mesenchymal stem cells (MSCs) were isolated from bone marrow collected from 20-month-old female C57BL/6 mice. The characteristics of MSCs were determined by morphology, surface markers, and multipotency (Figure S1), similar to our previous description [29].

For maintenance, mouse MSCs were grown in low-glucose DMEM (#31600034, Gibco, Waltham, MA, USA) supplemented with 10% fetal bovine serum (#10270106, Gibco) and 1% PSG (#10378016, Gibco). Osteogenic differentiation of MSCs was performed according to a previous study [29]. Briefly, MSCs were cultured in osteogenic induction medium with or without various GBE compounds, and the medium was changed every three days. Osteogenic induction medium consisted of high-glucose DMEM (#D7777, Sigma-Aldrich) supplemented with 0.1 μm dexamethasone (Sigma-Aldrich), 10 mM β-glycerol phosphate (#50020, Sigma-Aldrich), 0.2 mM ascorbic acid (#A8960, Sigma-Aldrich), and 1% PSG. Adipogenic medium consisted of DMEM supplemented with 1 μM dexamethasone, 50 μM indomethacin (#I7378, Sigma-Aldrich), 5 μg/mL insulin (#I2643, Sigma-Aldrich), 0.5 mM 3-isobutyl-1-methylxanthine (#I5879, Sigma-Aldrich), and 10% fetal bovine serum. Chondrogenic medium consisted of high-glucose DMEM supplemented with 0.1 μM dexamethasone, 50 μg/mL ascorbic acid, 100 μg/mL sodium pyruvate (#P5280, Sigma-Aldrich), 40 μg/mL L-proline (#P0380, Sigma-Aldrich), 10 ng/mL hTGFβ1 (#240-B, R&D Systems, Inc., Minneapolis, MN, USA), and 50 mg/mL ITS^{+} premix (#354352, BD Biosciences, San Jose, CA, USA). Monocytes were isolated from 20-month-old female C57BL/6 mice and differentiated into macrophages in RPMI 1640 (#11875085, Gibco) supplemented with 10% FBS and 20 ng/mL M-CSF (#315–02, PeproTech, Cranbury, NJ, USA). For osteoclastogenic induction, macrophages were cultured in α-MEM (#12000022, Gibco) supplemented with 10% FBS, M-CSF 50 ng/mL, RANKL 50 ng/mL (#315–11, PeproTech), and 1% PSG with or without 5 mg/L GB, and the induction medium was changed every three to seven days. For the H_2O_2 experiment, osteoclasts were treated with 5 mg/L GB 24 h prior to treatment with 300 μM H_2O_2 for 24 h.

2.7. Flow cytometry

For surface phenotyping, mouse MSCs were stained with CD29 (#562801), CD34 (#551387), CD44 (#553134), CD45 (#561087), CD105 (#562759), CD117 (#561075), CD73 (#567215) and CD31 (#558738) antibodies (BD Biosciences) and were analyzed by using flow cytometry (FACScan flow cytometer; Becton Dickinson). The results were visualized by FlowJo version 10 (BD Biosciences).

2.8. RNA isolation and gene expression analysis

RNA was isolated by using TRIzol® reagent (#15596018, Invitrogen, Grand Island, NY, USA) and reverse transcribed by High-Capacity cDNA Reverse Transcription Kit (#4368814, Thermo Fisher Scientific). Real-time PCR was performed using a StepOnePlus™ Real-time PCR System (Applied Biosystems, Foster City, CA, USA). The primers are listed in Table S1.

2.9. Alkaline phosphatase, Alizarin red S, tartrate-resistant acid phosphatase, and F-actin staining

For alkaline phosphatase histochemistry, cell layers were fixed with 3.7% formaldehyde, washed with distilled water (ddH2O), and stained with BCIP/NBT (5-bromo-4-chloro-3-indolyl phosphate/nitroblue tetrazolium, #B1911, Sigma-Aldrich) solution for 30 min in the dark at room temperature. ALP activity was measured using an ALP assay kit (#ab83369, Abcam Inc., Cambridge, UK) and normalized to the total protein content according to the manufacturer's instructions. To assess mineralized matrix, cells were fixed with 3.7% formaldehyde, washed with ddH2O and stained with 40 mM Alizarin red S solution (#A5533, Sigma-Aldrich) for 30 min at room temperature, and the stain was extracted by acetic acid and semiquantified as previously described [30]. For tartrate-resistant acid phosphatase (TRAP) staining, cells were fixed and stained with an acid phosphatase leukocyte assay kit (#387A, Sigma-Aldrich) according to the manufacturer's instructions. TRAP-positive cells with three or more nuclei were counted as osteoclasts. Fluor 488-labeled phalloidin (#A12379, Invitrogen) was used to stain F-actin. The average area and number of osteoclasts and nuclei per multinucleated cell were measured following phalloidin or TRAP staining.

2.10. Cell viability assay

Cells were treated with GB for 48 h, and cell viability was determined by a CCK-8 kit (#ab228554, Abcam).

2.11. ELISA analysis of OPG, RANKL and OCN

The expression levels of OPG and RANKL were quantified by ELISA (#EMTNFRSF11B and #EMTNFSF11, Invitrogen) and analyzed by a microplate reader (TECAN, Männedorf, Switzerland).

2.12. ROS and SOD activity measurement

Total ROS and superoxide were measured by a ROS/Superoxide Detection Assay kit (#ab139476, Abcam), and SOD activity was determined by Superoxide Dismutase Activity Assay Kit (#ab65354, Abcam) according to the manufacturer's instructions.

2.13. siRNA transfection

Control siRNA (#SIC001, 50 nM, Sigma-Aldrich) and target siRNA were transfected with RNAiMAX transfection reagent (#13778150, Invitrogen). After 18 h of transfection, the cells were washed with PBS, and the medium was replaced with fresh medium as appropriate. The siRNA sequences used were siSod2: UAUACUGAAGGUAGUAAGC and siCat: UGGCUAUGGAUAAAGGAUG.

2.14. Statistical analysis

Quantitative data are presented as the means ± SD in histograms with data points. Statistical analyses were performed using one-way ANOVA, two-way ANOVA or Student's t-test by GraphPad Prism 8 (GraphPad Software, Inc.) depending on the experimental design. A value of $P < 0.05$ was considered statistically significant.

2.15. Data availability statement

The LC-MS/MS data have been deposited in the ProteomeXchange Consortium (http://proteomecentral.proteomexchange.org) with the identifier PXD020328.

2.16. Study approval

All animal experiments were approved by the University Animal Experimentation Ethics Committee of the Chinese University of Hong Kong.

3. Results

3.1. GB is an effective component of GBE that increases the expression of osteogenic-specific genes

To confirm whether GB was the bioactive component of GBE that affected the osteoblastic phenotype, we treated aged MSC-derived osteoblasts with four structure-related *Ginkgo biloba*-specific terpenoids, including bilobalide, ginkgolide B, ginkgolide C, and ginkgolide J, and GBE for 48 h. MSCs were isolated from 20-month-old Balb/c mice, and the characteristics are shown in Figure S1. Compared with the control group, the GB treatment group exhibited upregulation of osteogenic-specific genes, including *Alpl*, *Sp7*, *Col1a1*, and *Bglap*, which was similar to the response to GBE treatment, suggesting that GB is the

bioactive component in GBE that mediates osteogenesis (Fig. 1 and S2).

3.2. GB alleviates OVX-induced osteoporosis

To verify whether oral gavage of GB improves postmenopausal osteoporosis, we treated OVX mice with two doses of GB daily (3 and 12 mg/kg body weight) for two months (Fig. 2A). The doses of GB used in mice were equivalent to the human doses of 0.3 and 1.2 mg/kg body weight [31]. Oral gavage of GB reduced body weight (Fig. 2B) and fat mass and increased lean mass in a dose-dependent manner compared with those of the OVX + vehicle group (Fig. 2C). Compared with those of the other groups, significant improvements in BMD and bone quality (Fig. 2D–G) were observed in high-dose GB-treated mice, while the effects of low-dose GB showed a trend toward significance (Fig. 2D–G). High-dose GB decreased circulating RANKL and increased the OPG-to-RANKL ratio compared with those of vehicle-treated OVX mice (Fig. 2H). Consistent with a previous study using an intraperitoneal injection approach [23], oral gavage of GB restored bone mass in estrogen-deficient mice.

3.3. GB attenuates osteoporosis in aged mice

To evaluate the therapeutic potential of GB in the treatment of aging-related osteoporosis, we administered GB (12 mg/kg body weight) to aged mice (20 months old) by oral gavage for two months (Fig. 3A). Compared with vehicle-treated aged mice, GB-treated mice exhibited decreases in body weight (Fig. 3B), white adipose tissue (Fig. 3C), and fat accumulation and an increase in lean mass (Fig. 3D). GB improved BMD (Fig. 3E) and many microarchitectural parameters of trabecular bone, such as bone surface density, bone-specific surface and trabecular thickness (Fig. 3F and G), and increased cortical bone thickness (Fig. 3H) in aged mice compared with vehicle-treated aged mice. Given the dysregulation of the OPG-RANK-RANKL system in the bone microenvironment during aging, we sought to investigate whether GB ameliorated the OPG-RANK-RANKL system in aged mice. Compared with those of their counterparts, GB decreased serum RANKL expression in GB-treated aged mice but did not alter OPG expression, leading to an increase in the OPG-to-RANKL ratio (Fig. 3I) and indicating that GB has systemic osteoanabolic and anti-osteocatabolic effects in aged mice. On the other hand, the regulation of the OPG-to-RANKL ratio suggested the involvement of GB in osteoblast-to-osteoclast communication.

3.4. GB does not induce adverse effects on the liver or kidney in aged mice

Aging is inexorably associated with impairments in various tissues and vulnerability to diseases [32,33]. To confirm whether GB treatment was safe for use in aged mice, we examined changes in the liver and kidney, the two primary organs involved in drug metabolism, in aged mice after GB treatment. We did not observe hepatic or renal histological alterations in GB-treated aged mice compared with their counterparts (Figure S3A). Moreover, there were no apparent adverse effects on liver or kidney functions, total cholesterol, or triglyceride levels in aged mice after GB treatment (Figure S3B). No tumors were observed in vehicle-treated or GB-treated mice. In summary, these results provide evidence that GB is safe for use in natural aging animals.

3.5. GB mitigates glucocorticoids-induced bone loss

Endogenous glucocorticoid levels increase with age, causing a deterioration in bone mass [34,35]. To verify whether GB improves glucocorticoid-induced osteoporosis, we injected Dex at a supra-physiologic dose (20 mg/kg body weight) daily into female C57BL/6 mice for 10 days, and then Dex-induced mice were untreated or administered GB with continued Dex injection for an additional 14 days. Dex injection resulted in marked bone loss in mice (Fig. 4A and B). Consistent with previous experiments, GB significantly improved BMD (Fig. 4A) and trabecular bone microarchitecture (Fig. 4B) in Dex-induced mice compared with untreated Dex-induced mice.

3.6. GB enhances bone quality under steady-state conditions

The prevention of osteoporosis is a primary area of research activity. Peak bone mass occurs during adulthood, typically plateaus for a period of time, and is associated with a reduced risk of osteoporosis during aging [36]. This finding indicated that increasing peak bone mass in early adulthood could prevent osteoporosis during aging. To evaluate whether GB affects bone mass under steady-state conditions, we administered GB to 6-month-old mice, which were approximately equivalent to humans ranging from 30 years of age [37,38], daily for two months. In general, GB significantly reinforced BMD (Fig. 5A) and

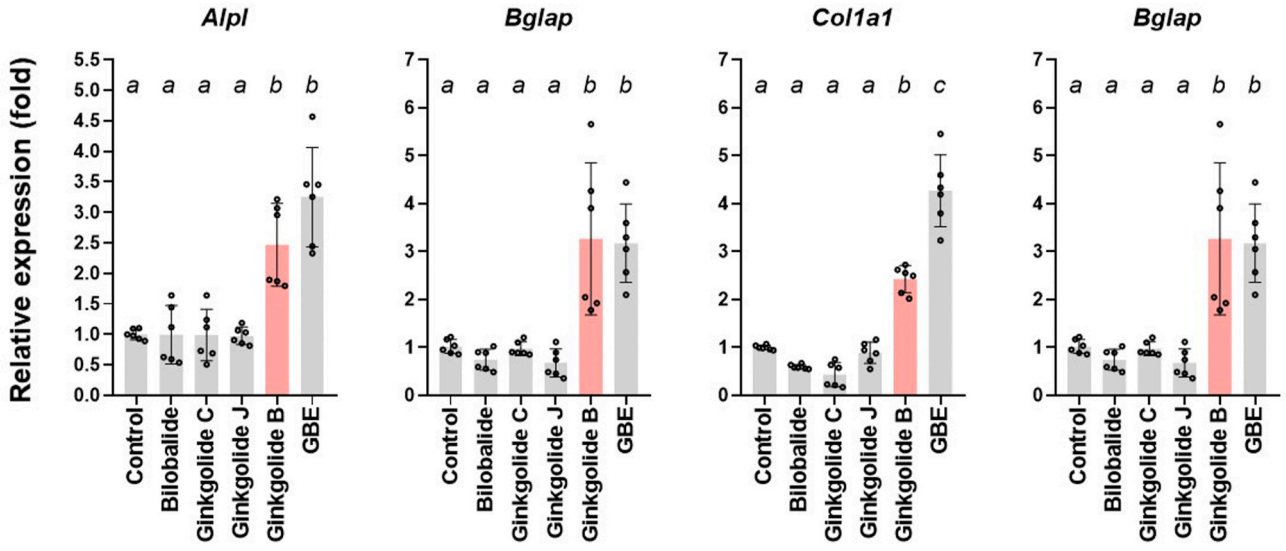

Fig. 1. GB increases the expression of osteogenic-specific genes in MSC-derived osteoblasts. qRT-PCR analysis of osteogenic-specific genes in MSC-derived osteoblasts after treatment with different components of GBE for 48 h (n = 6). Bilobalide, 1 mg/L; ginkgolide C, 20 mg/L; ginkgolide J, 20 mg/L; ginkgolide B 5 mg/L. Gene expression was normalized to that of the vehicle control group. Quantitative data are presented as the means ± SD in the histogram with data points. Statistical analyses were performed using one-way ANOVA with Tukey's multiple comparison test. Means that do not share any letters are significantly different ($p < 0.05$).

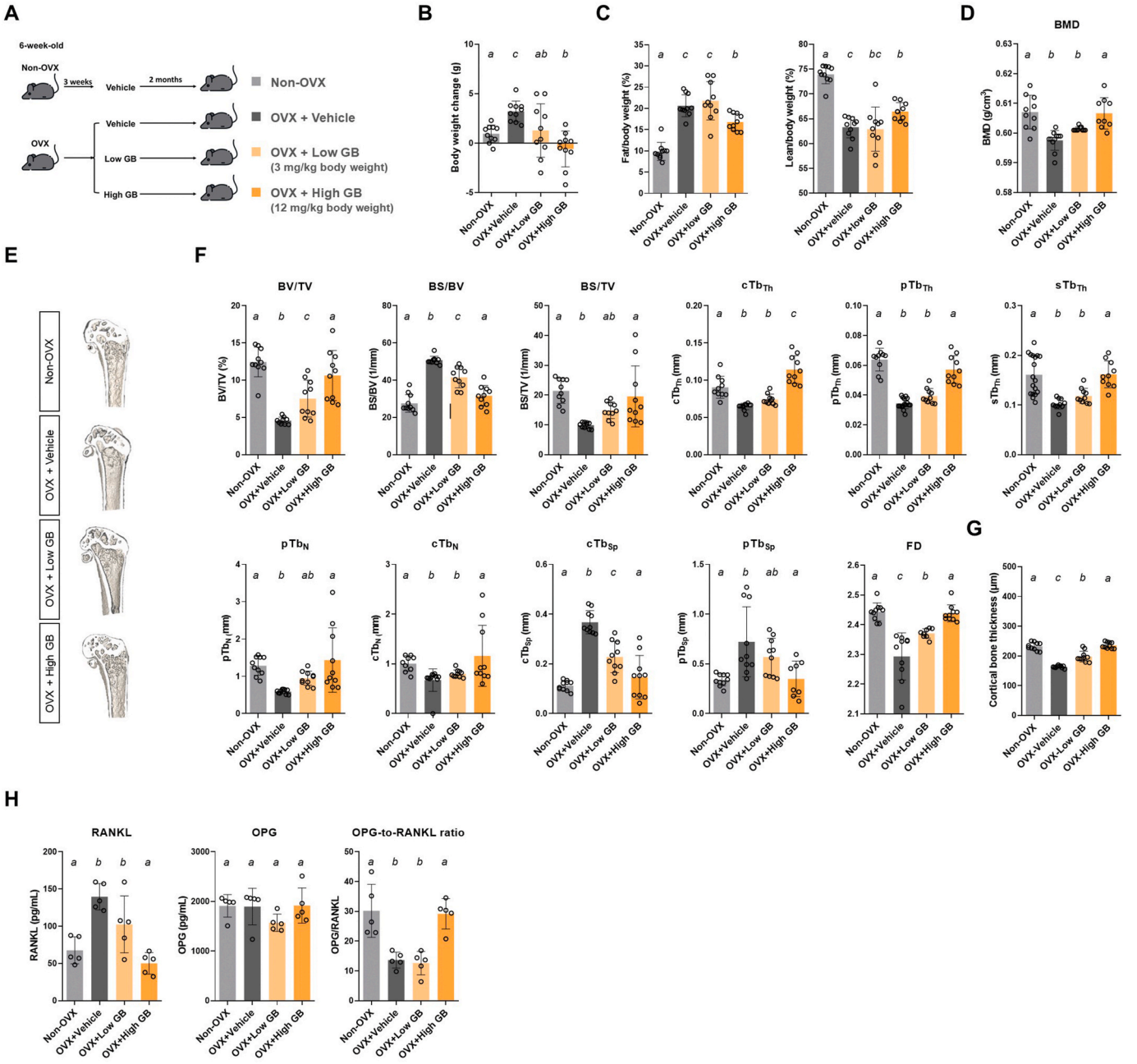

Fig. 2. GB ameliorates OVX-induced osteosarcopenia. (A) Experimental design. (B–C) Changes in body weight and (C) body composition after GB administration to OVX mice for two months (n = 10). (D–F) BMD (D), representative μCT images (E), and quantification of μCT-derived morphological parameters of the proximal femur (F) (n = 20 femur from 10 mice). (G) Quantification of cortical thickness of the femur. (H) The expression of serum RANKL and OPG revealed by ELISA (n = 5). BS, bone surface area; BV, bone volume; TV, tissue volume; BS/TV, bone surface density; BS/BV, bone specific surface; BV/TV, percentage bone volume; $_{c}Tb_{Th}$, $_{p}Tb_{Th}$ and sTb_{Th}, trabecular thickness (cylinder, plate, and sphere types, respectively); cTb_{N} and pTb_{N}, trabecular number (cylinder and plate types, respectively); cTb_{Sp} and pTb_{Sp}, trabecular separation (cylinder and plate types, respectively); FD, fractal dimension; $Cortical_{th}$, cortical thickness. Quantitative data are presented as the means ± SD in the histogram with data point. Statistical analyses are performed using one-way ANOVA with Tukey's multiple comparison test. Means not share any letter are significantly different ($p < 0.05$).

trabecular bone microarchitecture (Fig. 5B). Under steady-state conditions, GB treatment consistently increased bone quality, suggesting an opportunity for intervention in early adulthood. Taken together, our results demonstrated that oral gavage of GB exerts bone-protective effects in multiple animal models.

3.7. GB restores bone homeostasis in aged cells

Evidence shows that deterioration in MSC viability, proliferation and osteogenic differentiation and increases in the osteoclast progenitor pool and osteoclastogenesis during aging result in the development of osteoporosis [4–7]. We next elucidated whether GB directly affects the cellular behaviors of aged MSCs and aged macrophages, the osteoclast progenitors. GB did not affect cell viability or the expression of the proliferation marker *Ki67* in aged MSCs, osteoblasts, macrophages, or osteoclasts (Figure S4A-D). We then investigated the role of GB in osteogenesis and osteoclastogenesis in aged cells. Compared with vehicle control (OB group), GB treatment throughout osteogenic induction upregulated osteoblastic early-stage (*Runx2* and *Alpl*), middle-stage (*Sp7*) and late-stage indicators (*Bglap* and *Col1a1*)

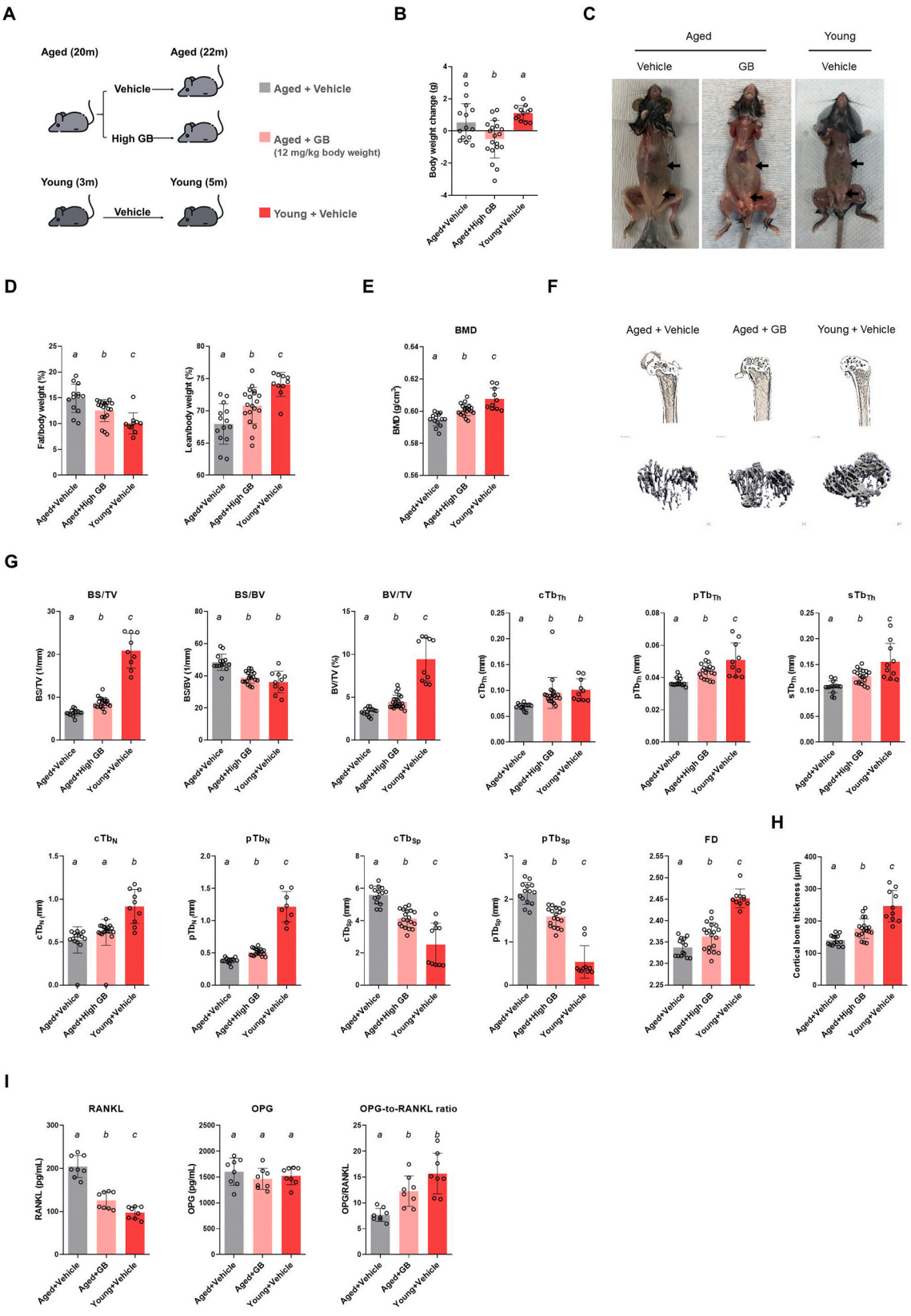

Fig. 3. GB is an effective component for treating aging-related osteoporosis. (A) Experimental design: Aged C57BL/6 mice (20 months old) received GB or vehicle daily by oral gavage for two months and young mice (3 months old) received vehicle daily by oral gavage for two months (Aged + Vehicle, n = 14; Aged + GB, n = 19; Young + Vehicle, n = 10). (B–D) Changes in body weight (B), representative photographs (C), and body composition (D) after GB administration to aged mice for two months. The arrow in (C) indicates the adipose tissue. (E) BMD of the proximal femur. (F) Representative μCT images of the proximal femur. (G) Quantification of μCT-derived proximal femur morphological parameters. (H) Quantification of cortical thickness. (I) Serum levels of OPG and RANKL were measured by ELISA (n = 8). Quantitative data are presented as the means ± SD in the histogram with data points. Statistical analyses were performed using one-way ANOVA with Tukey's multiple comparison test. Means that do not share any letters are significantly different ($p < 0.05$).

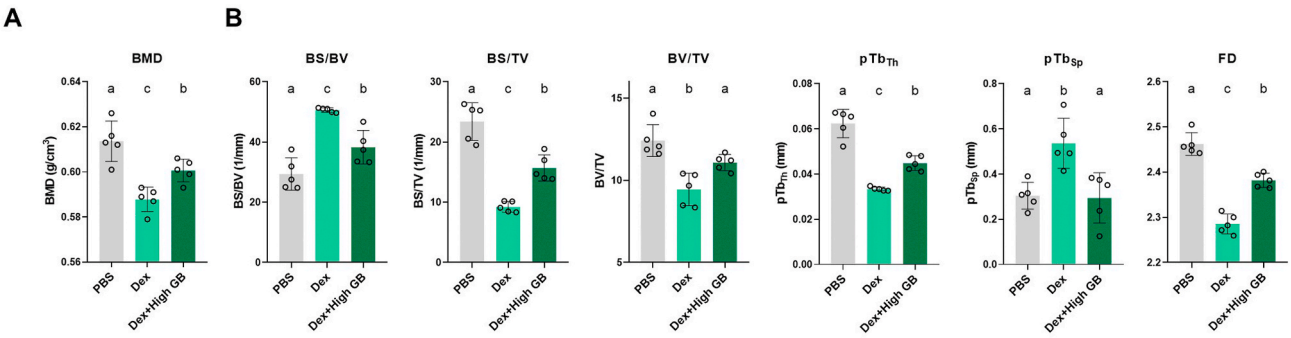

Fig. 4. GB improves glucocorticoid-induced bone loss. C57BL/6 mice (6 weeks old) received Dex by IP injection and GB daily by oral gavage. (A) BMD of the proximal femur. (B) The trabecular bone phenotype in the proximal femur was quantified by μCT (n = 5 for each group). BS/TV, bone surface density; BS/BV, bone-specific surface; BV/TV, percentage bone volume; pTb$_{Th}$, trabecular thickness (plate type); pTb$_{Sp}$, trabecular separation (plate type); FD, fractal dimension; Cortical$_{th}$, cortical thickness. Quantitative data are presented as the means ± SD in the histogram with the data points. Statistical analyses were performed using one-way ANOVA with Tukey's multiple comparison test. Means that do not share any letters are significantly different ($p < 0.05$).

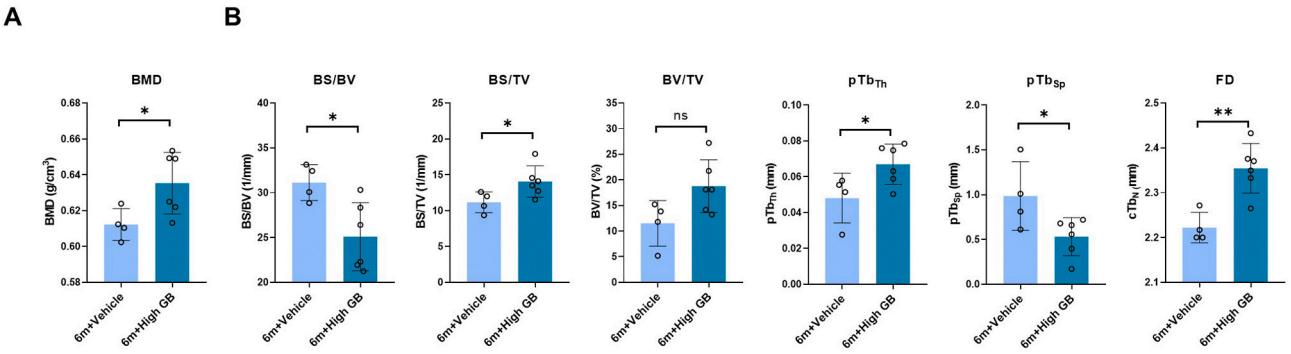

Fig. 5. GB increases bone mass under steady-state conditions. C57BL/6 mice (6 months old) received GB daily by oral gavage for two months. (A) BMD of the proximal femur. (B) Quantification of μCT-derived proximal femur morphological parameters (n = 4 for the vehicle group; n = 6 for the GB group). BS/TV, bone surface density; BS/BV, bone-specific surface; BV/TV, percentage bone volume; pTb$_{Th}$, trabecular thickness (plate type); pTb$_{Sp}$, trabecular separation (plate type); FD, fractal dimension; Cortical$_{th}$, cortical thickness. Quantitative data are presented as the means ± SD in the histogram with the data points. Statistical analyses were performed using Student's t-test, with significance set at $P < 0.05$. (*$P < 0.05$; **$P < 0.01$).

(Fig. 6A), enhanced ALP activity at OD day 3 (Fig. 6B), and increased matrix mineralization at day 9 (Fig. 6C). Our results indicated that GB promoted osteogenesis in aged MSCs. Osteoclastogenic differentiation of aged macrophages was evidenced by the upregulation of osteoclastogenic-specific genes, including *Acp5*, *Ctsk*, *Mmp9*, *Nfatc1*, and *Oscar* (Fig. 6D). GB markedly downregulated osteoclastogenesis-specific genes (Fig. 6E) and reduced the numbers of multinucleated cells (Fig. 6F) and TRAP-positive cells (Fig. 6G). The number of nuclei and area of multinucleated cells were decreased after GB treatment, indicating the inhibition of cell-cell fusion and osteoclast maturation (Fig. 6H).

Consistent with the in vivo results, we found that GB decreased the transcript and protein levels of RANKL in aged MSCs (Fig. 7A and B) and aged osteoblasts (Fig. 7C and D), leading to an increase in the OPG-to-RANKL ratio, while GB did not affect the expression of *Rank* in aged macrophages or aged osteoclasts (Fig. 7E). Taken together, these results suggest that GB possesses bone formation properties and inhibits bone resorption in aged cells to ameliorate osteoporosis.

3.8. GB modulates the circulating proteomic profile in naturally aged mice

Aging-related osteoporosis is associated with changes in circulating factors, and circulation rejuvenation can improve stem cell activity and bone quality in aged mice [39]. To clearly and comprehensively characterize the serum protein profile of GB-treated aged mice, a label-free proteomics approach using LC-MS/MS was used. A total of 347 proteins were identified as differentially expressed proteins (DEPs) between the young and aged groups (Table S2), 47 proteins were identified as DEPs between the aged + vehicle and aged + GB groups (Table S3), and 17 DEPs were identified in both datasets (Fig. 8A). The hierarchical clustering heatmap revealed that GB partially shifted the serum DEP profile of aged mice toward that of young mice (Fig. 8B). Gene Ontology classification showed that the DEPs in the two datasets (young vs. aged and aged vs. aged + GB) were associated with similar annotations, which suggested commonly altered functional pathways in the serum protein profile (Fig. 8C). Regarding biological processes, DEPs between the aged + vehicle and aged + GB groups were related to cellular processes, immune system processes, and metabolic processes (Fig. 8C, left panel). The top two DEPs associated with cellular components were related to the extracellular region and membrane (Fig. 8C, middle panel). Most DEPs associated with molecular functions were related to binding and catalytic activity (Fig. 8C, right panel). Furthermore, gene ontology analysis revealed 149 different GO terms associated with DEPs between the aged + vehicle and aged + GB groups that were highly associated with the inflammatory response, aging, and oxidative stress pathways (Fig. 8D).

3.9. ROS mediate the effects of GB on osteogenic and osteoclastogenic differentiation

Oxidative stress is a hallmark of aging and is also associated with various pathological conditions. The aging-related increase in oxidative stress is attributed to the downregulation of ROS scavengers in bone [10] which dysregulates bone homeostasis and leads to osteoporosis

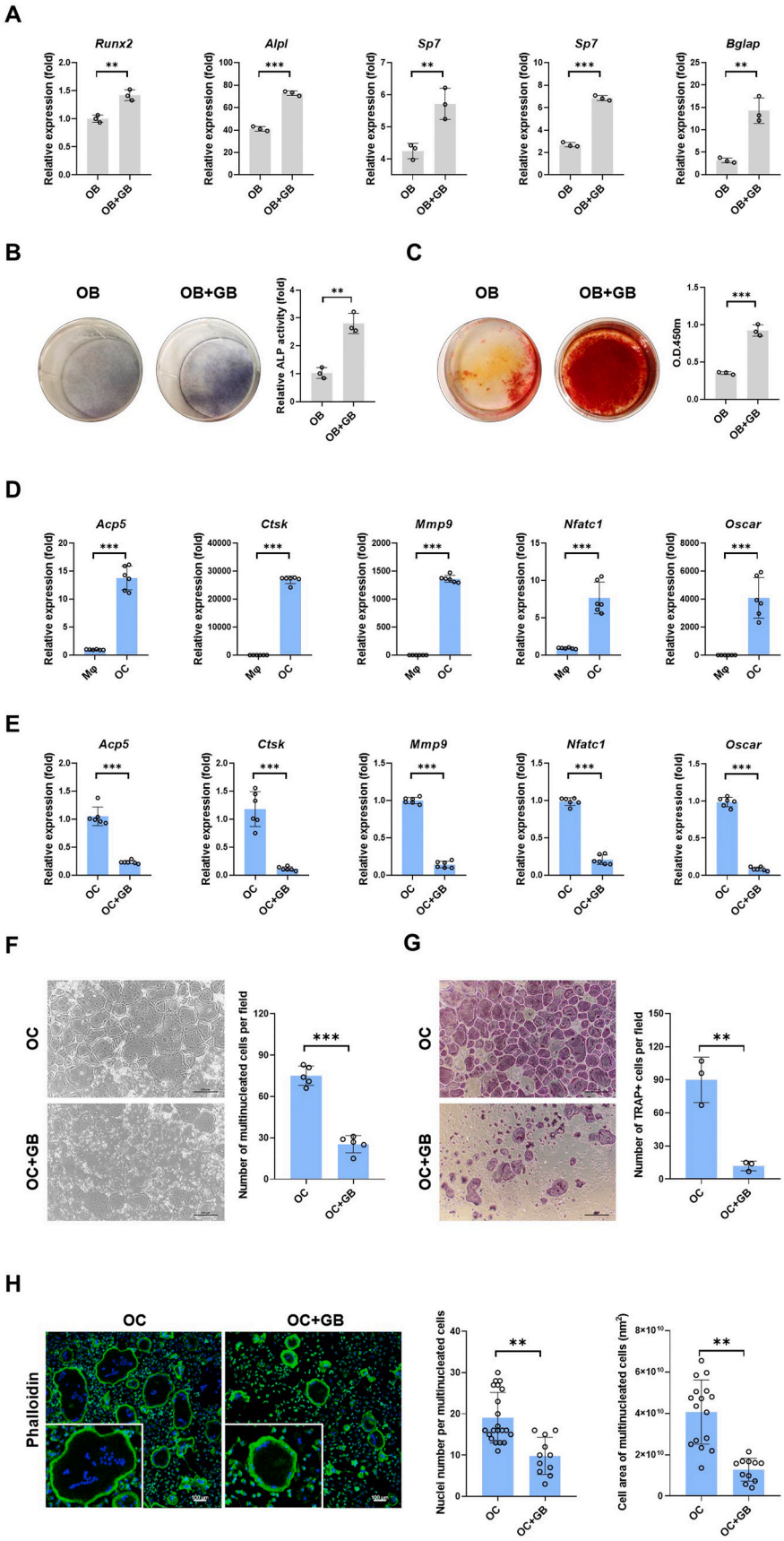

Fig. 6. GB promotes the osteogenic differentiation of aged MSCs and represses the osteoclastogenic differentiation of aged macrophages in culture. (A) Expression of osteogenic-specific genes at osteogenic differentiation day 6 (n = 6). Gene expression was normalized to that of undifferentiated MSCs. (B) Alkaline phosphatase staining and activity in aged MSCs at osteogenic differentiation day 3 with or without GB. (C) Alizarin red S staining of aged MSCs at osteogenic differentiation day 9 with or without GB. (D) The expression of osteoclastogenic-specific genes at osteoclastogenic differentiation day 7 (n = 6). (E) The expression of osteoclastogenic-specific genes at osteoclastogenic differentiation day 7 with GB treatment (n = 6). (F) Representative cellular morphology. The number of multinucleated cells (≥3 nuclei) was quantified (n = 5). (G) Representative TRAP staining. The number of TRAP-positive multinucleated cells (≥3 nuclei) was quantified (n = 3). (H) Phalloidin staining of F-actin and DAPI staining of nuclei. The number of nuclei and cell areas of multinucleated cells were quantified (n = 10). Scale bar in (F) and (G): 500 μm; scale bar in (H): 100 μm. GB, ginkgolide B (5 mg/L); Mϕ, macrophage; OB, MSC-derived osteoblast; OC, macrophage-derived osteoclast. Quantitative data are presented as the means ± SD in the histogram with the data points. Statistical analyses were performed using Student's t-test, with significance set at $P < 0.05$. (*$P < 0.05$; **$P < 0.01$; ***$P < 0.001$). (For interpretation of the references to colour in this figure legend, the reader is referred to the Web version of this article.)

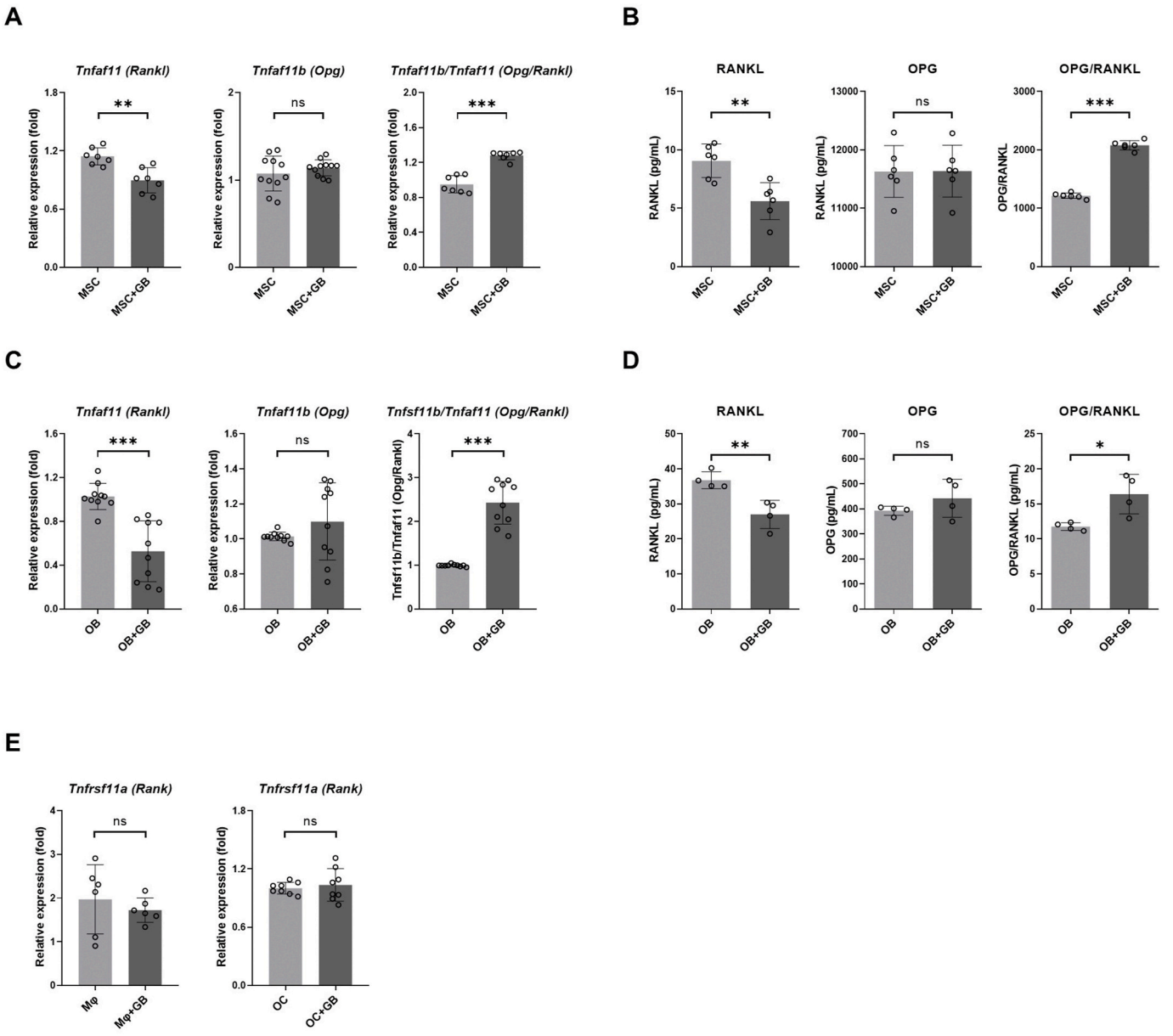

Fig. 7. GB increases the OPG-to-RANKL ratio in MSCs and osteoblasts from aged mice. (A–B) The expression of OPG and RANKL in aged MSCs was measured by qRT-PCR (n = 7) (A) and ELISA (n = 6) (B). (C–D) The expression of OPG and RANKL in aged osteoblasts was measured by qRT-PCR (n = 10) (C) and ELISA (n = 4) (D). (E) RANK expression in aged macrophages and aged osteoclasts was measured by qRT-PCR (n = 6). Statistical analyses were performed using Student's t-test, with significance set at $P < 0.05$. (*$P < 0.05$; **$P < 0.01$; ***$P < 0.001$; ns, not significant).

during aging [11]. Given the serum DEPs of GB-treated aged mice were correlated with oxidative stress (Fig. 8D), we sought to determine whether GB modulates bone metabolism by inhibiting ROS. GB decreased total ROS and superoxide levels in both aged MSCs and MSC-derived osteoblasts (Fig. 9A and B) and upregulated the ROS scavengers *catalase* and *Sod2* but not *Sod1* during OD (Fig. 9C). GB enhanced SOD activity during osteogenic differentiation of aged MSCs (Figure S5). Knockdown of *catalase* and *Sod2* reduced *catalase* and *Sod2* in osteoblasts, and there was no compensatory upregulation of *Sod1* after knockdown of catalase and Sod2 knockdown (Fig. 9D). Knockdown of *catalase* and *Sod2* in GB-treated osteoblasts markedly decreased osteogenic-specific genes and increased *Rankl* expression (Fig. 9E). In addition, GB also decreased the levels of total ROS and superoxide in aged macrophages and osteoclasts (Fig. 9F and G). Although GB did not alter the levels of *catalase*, *Sod1,* or *Sod2* during osteoclastogenesis (Fig. 9H), GB abolished the promotion of osteoclastogenesis induced by exogenous H_2O_2 treatment (Fig. 9I and J). In summary, our results indicate that GB regulates osteogenic differentiation and osteoclastogenic differentiation through the inhibition of ROS in aged cells.

4. Discussion

Osteoporosis is associated with falls and fractures that increase the risk of immobility and institutionalization. For years, conventional osteoporosis treatment has involved either the inhibition of bone resorption or the promotion of bone formation [40], and is associated with unexpected adverse side effects. Increasing evidence reveals that GB exerts protective effects against aging-related diseases [41–46]. In this study, we demonstrated the bone-protective effects of orally administered GB on various animal models, including aging, postmenopausal, iatrogenic and healthy mice. GB has dual effects on bone homeostasis, such as promoting osteogenesis, repressing

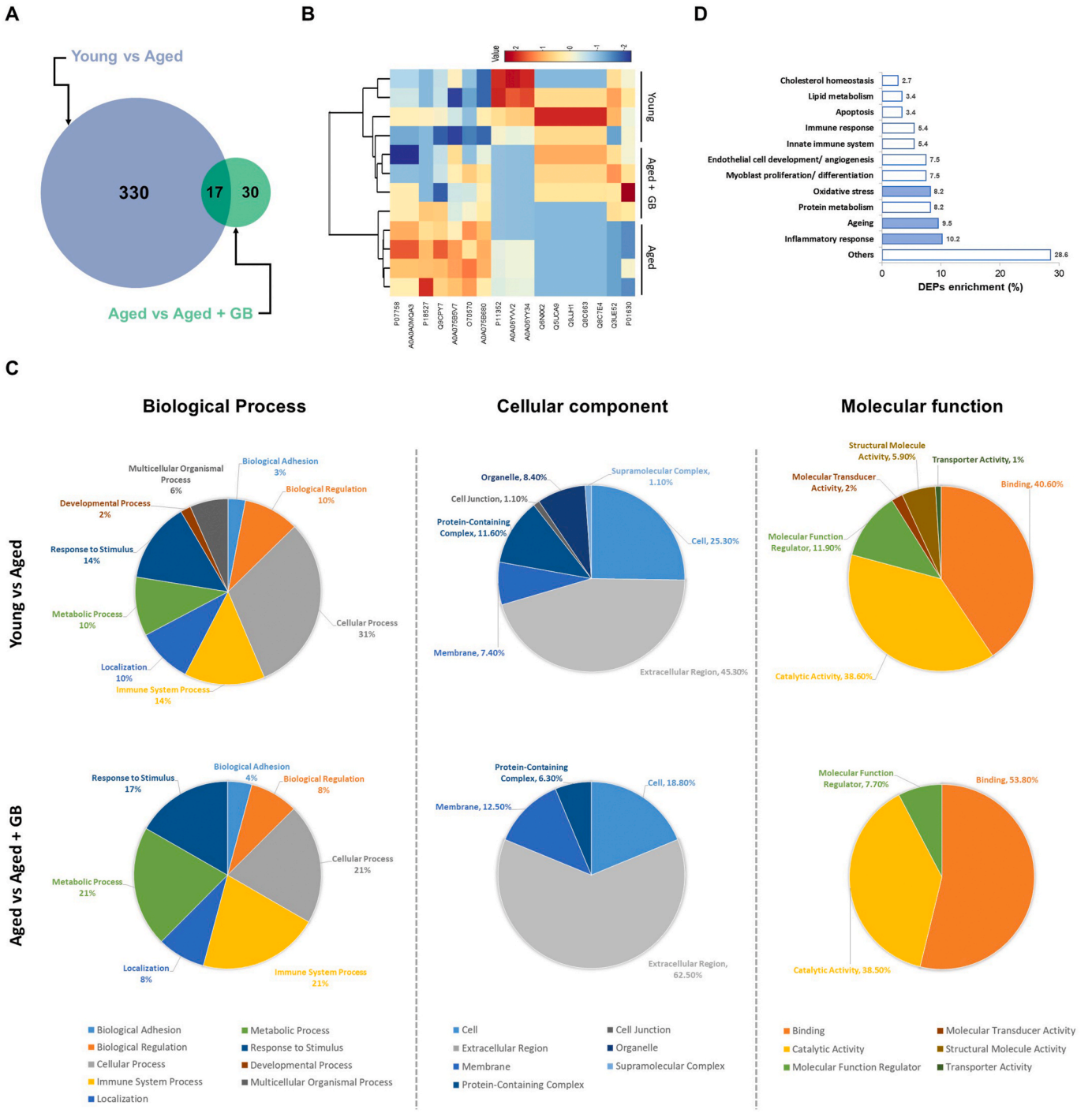

Fig. 8. Serum protein profile of aged mice with or without GB administration. (A) Venn diagrams of the DEPs between the two serum datasets (n = 4). (B) Hierarchical clustering analysis of a heatmap of the DEPs between young, aged, and aged + GB groups. (C) Functional classifications of the differentially expressed proteins (DEPs) between young, aged, and aged + GB groups according to their biological processes, cellular components, and molecular functions. The categorizations were analyzed by the PANTHER online tool system. (D) Gene ontology enrichment analysis of the DEPs between the aged and aged + GB groups. The DEP list was obtained using a 1.5-fold cutoff, a false discovery rate of <1%, and a significance threshold of $p < 0.05$.

osteoclastogenesis, and increasing the OPG-to-RANKL ratio.

A progressive and continuous increase in ROS was observed in aged C57BL/6 mice [11], postmenopausal mice [47] and glucocorticoid-treated mice [48], together with the loss of bone mass. Deficiencies in ROS scavengers abolishes osteogenic activity [49] and promote osteoclast generation [50] to induce osteoporosis. GB treatment partially abrogated the aging-related changes in circulating molecules associated with oxidative stress, inflammation, and the aging process. Indeed, GB reduced ROS by upregulating the ROS scavengers *Sod2* and *catalase* to enhance osteogenic differentiation in aged MSCs. Knockdown of *Sod2* and *catalase* abolished GB-mediated promotion of osteogenesis. A previous study showed that GB activated canonical Wnt signaling in MSCs to promote osteoblast differentiation, and intraperitoneal injection of GB improved bone mass in OVX mice [23]. Aging-related increases in ROS suppress osteogenesis by antagonizing the Wnt/β-catenin/TCF pathway [12], suggesting that GB might regulate Wnt/β-catenin signaling via ROS inhibition. In addition, ROS have been shown to mediate RANKL-induced osteoclastogenic differentiation

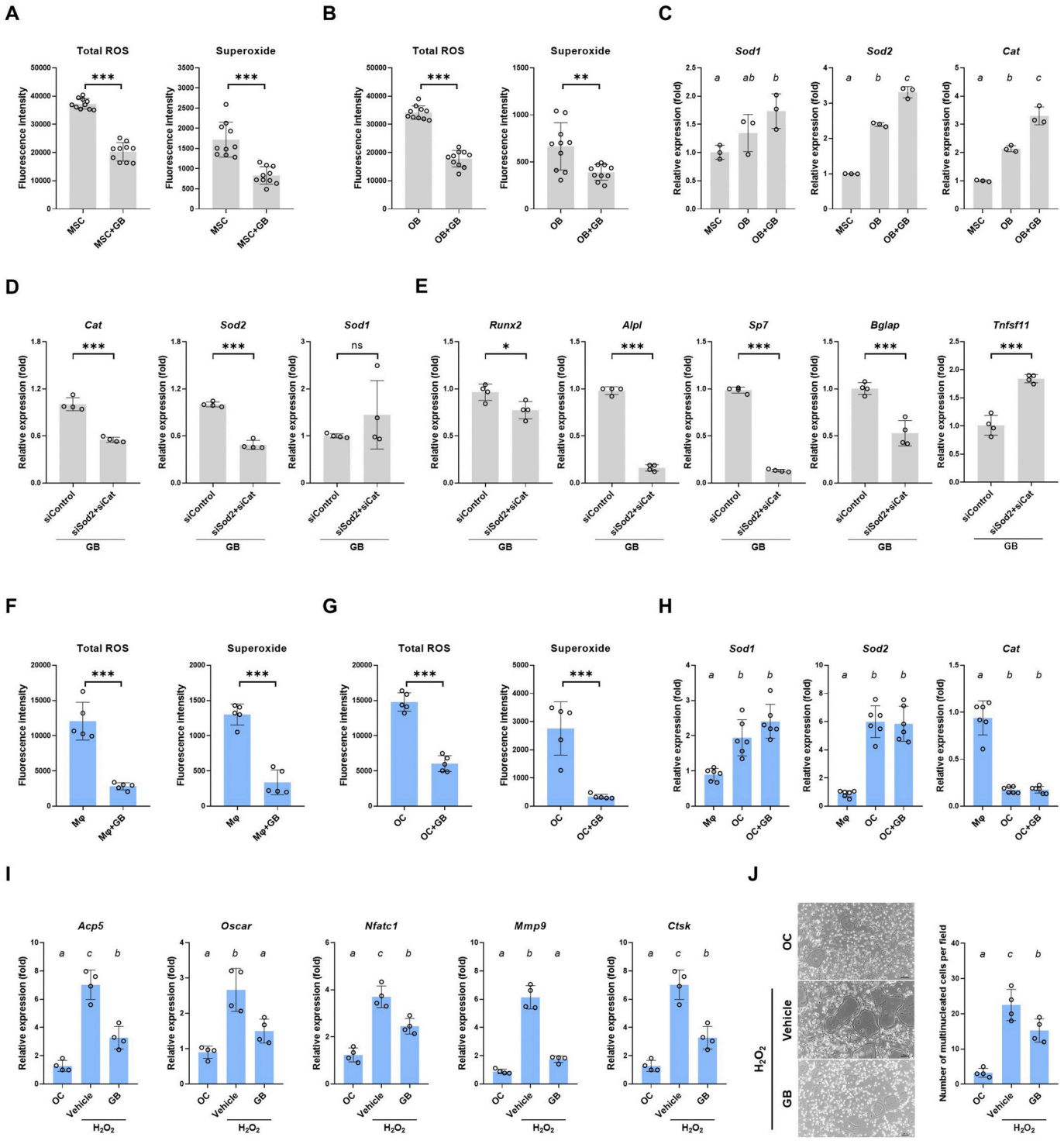

Fig. 9. GB decreases reactive oxygen species to regulate osteogenic differentiation and osteoclastogenic differentiation in aged cells. (A–B) GB decreased the levels of ROS in aged MSCs (A) and aged MSC-derived osteoblasts (B) (n = 10). (C) The expression levels of catalase, Sod1, and Sod2 in aged MSC-derived osteoblasts after GB treatment were measured by qRT-PCR (n = 3). (D) The expression levels of catalase, Sod1 and Sod2 after siRNA transfection in aged MSC-derived osteoblasts were measured by qRT-PCR (n = 4). (E) Knockdown of catalase and Sod2 attenuated the effect of GB on osteogenic-specific genes in aged MSC-derived osteoblasts, as indicated by qRT-PCR (n = 4). (F–G) GB decreased the levels of superoxide and total ROS in aged macrophages (F) and aged macrophage-derived osteoclasts (G). (H) The expression levels of catalase, Sod1, and Sod2 in aged macrophages and aged macrophage-derived osteoclasts was measured by qRT-PCR (n = 3). (I–J) The expression of osteoclastogenic-specific genes (n = 4) (I) and number of multinucleated cells (≥3 nuclei) (n = 3) (J) at osteoclastogenic differentiation day 4 with H_2O_2 and GB treatment. GB, ginkgolide B (5 mg/L); Mϕ, macrophage; OC, macrophage-derived osteoclast. Statistical analyses were performed using Student's t-test, with significance set at $P < 0.05$. (*$P < 0.05$; **$P < 0.01$; ***$P < 0.001$; ns, not significant) or using one-way ANOVA with Tukey's multiple comparison test (means that do not share any letters are significantly different ($p < 0.05$)), depending on the experimental design.

[51]. In this study, we found that GB reduced ROS and inhibited RANKL-induced osteoclastogenic differentiation in aged macrophages, and GB also neutralized exogenous H_2O_2-induced promotion of osteoclastogenic differentiation. Thus, we suggest that GB represses osteoclast differentiation in a ROS-dependent manner. To the best of our knowledge, this is the first evidence that GB regulates osteoclastogenesis. Our results suggest that GB rebalances bone homeostasis by targeting ROS in aged mice with osteoporosis.

Aging-associated inflammation, or inflammaging, is associated with over-accusation of ROS in cells and plays a critical role in the pathogenesis of most aging-related diseases [52,53]. Although inhibiting inflammation is an unequivocal therapeutic approach to preventing and treating aging-related osteoporosis, the development of effective treatments is still a challenge for researchers. We showed that serum DEPs related to the immune response and anti-inflammation were positively associated with improving bone mass in GB-treated aged mice. Our results suggest that GB might maintain bone homeostasis by exerting anti-inflammatory effects. On the other hand, GB treatment showed modest but consistent bone enhancement in steady-state conditions, which is not “inflammatory” in nature per se. Therefore, the therapeutic effect of GB is mediated not only by anti-inflammatory effects but also by direct effects on bone cells.

In summary, this study demonstrates that oral gavage of GB protects bone in aging, postmenopausal, iatrogenic osteoporotic conditions and steady-state conditions and underscores the rejuvenating effect of GB on circulating molecules. Since patients with osteoporosis require a long-term regimen, oral GB administration provides a convenient, reliable, and highly accessible method for sustained delivery. Understanding the detailed molecular mechanisms of how GB regulates oxidative stress and restores bone homeostasis will contribute to the application of GB for aging-related osteoporosis and other degenerative diseases and accelerate bench-to-bedside clinical translation.

Author contributions

Chien-Wei Lee performed experiments, analyzed the data and wrote the manuscript. Hui-Chu Lin, Belle Yu-Hsuan Wang, Amanda Yu-Fan Wang, Rita Lih-Ying Shin, and Stella YL Cheung performed experiments. Oscar Kuang-Sheng Lee designed and supervised the study. All authors have approved the final manuscript.

Declaration of competing interest

Chien-Wei Lee, Hui-Chu Lin, Belle Yu-Hsuan Wang, Amanda Yu-Fan Wang, Rita Lih-Ying Shin, Stella Yee Lo Cheung, and Oscar K. Lee declare that they have no conflicts of interest.

Acknowledgment

This work was supported by the MWLC Associate Member Programme, Ming Wai Lau Centre for Reparative Medicine of Karolinska Institute to OK Lee and the CUHK Research Committee Direct Grant for Research (Reference no. 2018.020) and Hong Kong Government Research Grant Council, General Research Fund (Reference no. 14104620) to CW Lee. The authors acknowledge technical support provided by the core facility of the School of Biomedical Sciences, Faculty of Medicine, the Chinese University of Hong Kong, Li Ka Shing Institute of Health Sciences, The Chinese University of Hong Kong, Prince of Wales Hospital. The authors declare no competing financial interests.

Appendix A. Supplementary data

Supplementary data to this article can be found online at https://doi.org/10.1016/j.freeradbiomed.2021.03.008.

References

[1] M.J. Prince, F. Wu, Y. Guo, L.M. Gutierrez Robledo, M. O'Donnell, R. Sullivan, S. Yusuf, The burden of disease in older people and implications for health policy and practice, Lancet 385 (9967) (2015) 549–562.
[2] S.W. Tsang, A.W. Kung, J.A. Kanis, H. Johansson, A. Oden, Ten-year fracture probability in Hong Kong Southern Chinese according to age and BMD femoral neck T-scores, Osteoporos. Int. 20 (11) (2009) 1939–1945.
[3] C.H. Bow, E. Cheung, C.L. Cheung, S.M. Xiao, C. Loong, C. Soong, K.C. Tan, M. M. Luckey, J.A. Cauley, S. Fujiwara, A.W. Kung, Ethnic difference of clinical vertebral fracture risk, Osteoporos. Int. 23 (3) (2012) 879–885.
[4] E.J. Moerman, K. Teng, D.A. Lipschitz, B. Lecka-Czernik, Aging activates adipogenic and suppresses osteogenic programs in mesenchymal marrow stroma/stem cells: the role of PPAR-gamma2 transcription factor and TGF-beta/BMP signaling pathways, Aging Cell 3 (6) (2004) 379–389.
[5] C.J. Li, P. Cheng, M.K. Liang, Y.S. Chen, Q. Lu, J.Y. Wang, Z.Y. Xia, H.D. Zhou, X. Cao, H. Xie, E.Y. Liao, X.H. Luo, MicroRNA-188 regulates age-related switch between osteoblast and adipocyte differentiation, J. Clin. Invest. 125 (4) (2015) 1509–1522.
[6] S.L. Perkins, R. Gibbons, S. Kling, A.J. Kahn, Age-related bone loss in mice is associated with an increased osteoclast progenitor pool, Bone 15 (1) (1994) 65–72.
[7] P.L. Chung, S. Zhou, B. Eslami, L. Shen, M.S. LeBoff, J. Glowacki, Effect of age on regulation of human osteoclast differentiation, J. Cell. Biochem. 115 (8) (2014) 1412–1419.
[8] D.A. Callaway, J.X. Jiang, Reactive oxygen species and oxidative stress in osteoclastogenesis, skeletal aging and bone diseases, J. Bone Miner. Metabol. 33 (4) (2015) 359–370.
[9] V. Domazetovic, G. Marcucci, T. Iantomasi, M.L. Brandi, M.T. Vincenzini, Oxidative stress in bone remodeling: role of antioxidants, Clin Cases Miner Bone Metab 14 (2) (2017) 209–216.
[10] Y.Y. Hor, C.H. Ooi, L.C. Lew, M.H. Jaafar, A.S. Lau, B.K. Lee, A. Azlan, S.B. Choi, G. Azzam, M.T. Liong, The molecular mechanisms of probiotic strains in improving ageing bone and muscle of d-galactose-induced ageing rats, J. Appl. Microbiol. 130 (4) (2021) 1307–1322.
[11] M. Almeida, L. Han, M. Martin-Millan, L.I. Plotkin, S.A. Stewart, P.K. Roberson, S. Kousteni, C.A. O'Brien, T. Bellido, A.M. Parfitt, R.S. Weinstein, R.L. Jilka, S. C. Manolagas, Skeletal involution by age-associated oxidative stress and its acceleration by loss of sex steroids, J. Biol. Chem. 282 (37) (2007) 27285–27297.
[12] M. Almeida, L. Han, M. Martin-Millan, C.A. O'Brien, S.C. Manolagas, Oxidative stress antagonizes Wnt signaling in osteoblast precursors by diverting beta-catenin from T cell factor- to forkhead box O-mediated transcription, J. Biol. Chem. 282 (37) (2007) 27298–27305.
[13] W.S. Simonet, D.L. Lacey, C.R. Dunstan, M. Kelley, M.S. Chang, R. Luthy, H. Q. Nguyen, S. Wooden, L. Bennett, T. Boone, G. Shimamoto, M. DeRose, R. Elliott, A. Colombero, H.L. Tan, G. Trail, J. Sullivan, E. Davy, N. Bucay, L. Renshaw-Gegg, T.M. Hughes, D. Hill, W. Pattison, P. Campbell, S. Sander, G. Van, J. Tarpley, P. Derby, R. Lee, W.J. Boyle, Osteoprotegerin: a novel secreted protein involved in the regulation of bone density, Cell 89 (2) (1997) 309–319.
[14] D.L. Lacey, E. Timms, H.L. Tan, M.J. Kelley, C.R. Dunstan, T. Burgess, R. Elliott, A. Colombero, G. Elliott, S. Scully, H. Hsu, J. Sullivan, N. Hawkins, E. Davy, C. Capparelli, A. Eli, Y.X. Qian, S. Kaufman, I. Sarosi, V. Shalhoub, G. Senaldi, J. Guo, J. Delaney, W.J. Boyle, Osteoprotegerin ligand is a cytokine that regulates osteoclast differentiation and activation, Cell 93 (2) (1998) 165–176.
[15] G.A. Rodan, T.J. Martin, Therapeutic approaches to bone diseases, Science 289 (5484) (2000) 1508–1514.
[16] M.T. Drake, B.L. Clarke, S. Khosla, Bisphosphonates: mechanism of action and role in clinical practice, Mayo Clin. Proc. 83 (9) (2008) 1032–1045.
[17] I.R. Reid, Osteonecrosis of the jaw: who gets it, and why? Bone 44 (1) (2009) 4–10.
[18] Y. Liu, J.P. Liu, Y. Xia, Chinese herbal medicines for treating osteoporosis, Cochrane Database Syst. Rev. 3 (2014) CD005467.
[19] D. Lichtblau, J.M. Berger, K. Nakanishi, Efficient extraction of ginkgolides and bilobalide from Ginkgo biloba leaves, J. Nat. Prod. 65 (10) (2002) 1501–1504.
[20] W. Zuo, F. Yan, B. Zhang, J. Li, D. Mei, Advances in the studies of Ginkgo biloba leaves extract on aging-related diseases, Aging Dis 8 (6) (2017) 812–826.
[21] Y. Yang, J. Chen, Q. Gao, X. Shan, J. Wang, Z. Lv, Study on the attenuated effect of Ginkgolide B on ferroptosis in high fat diet induced nonalcoholic fatty liver disease, Toxicology 445 (2020) 152599.
[22] T. Wu, X. Fang, J. Xu, Y. Jiang, F. Cao, L. Zhao, Synergistic effects of ginkgolide B and protocatechuic acid on the treatment of Parkinson's disease, Molecules 25 (17) (2020).
[23] B. Zhu, F. Xue, C. Zhang, G. Li, Ginkgolide B promotes osteoblast differentiation via activation of canonical Wnt signalling and alleviates osteoporosis through a bone anabolic way, J. Cell Mol. Med. 23 (8) (2019) 5782–5793.
[24] S.V. Koebele, H.A. Bimonte-Nelson, Modeling menopause: the utility of rodents in translational behavioral endocrinology research, Maturitas 87 (2016) 5–17.
[25] C. Shen, X. Jin, M. Wu, X. Huang, J. Li, H. Huang, F. Li, J. Liu, G. Rong, S. Song, A sensitive LC-MS/MS method to determine ginkgolide B in human plasma and urine: application in a pharmacokinetics and excretion study of healthy Chinese subjects, Xenobiotica 50 (3) (2020) 323–331.
[26] F. Shao, H. Zhang, L. Xie, J. Chen, S. Zhou, J. Zhang, J. Lv, W. Hao, Y. Ma, Y. Liu, N. Ou, W. Xiao, Pharmacokinetics of ginkgolides A, B and K after single and multiple intravenous infusions and their interactions with midazolam in healthy Chinese male subjects, Eur. J. Clin. Pharmacol. 73 (5) (2017) 537–546.
[27] D.S.-C. Jin, C.-H. Chu, J.-C. Chen, Trabecular bone morphological analysis for preclinical osteoporosis application using micro computed tomography scanner, J. Med. Biol. Eng. 36 (1) (2016) 96–104.

[28] Y.L. Huang, Z.Q. Shen, C.Y. Wu, Y.C. Teng, C.C. Liao, C.H. Kao, L.K. Chen, C.H. Lin, T.F. Tsai, Comparative proteomic profiling reveals a role for Cisd2 in skeletal muscle aging, Aging Cell 17 (1) (2018).
[29] C.W. Lee, W.C. Huang, H.D. Huang, Y.H. Huang, J.H. Ho, M.H. Yang, V.W. Yang, O.K. Lee, DNA Methyltransferases Modulate Hepatogenic Lineage Plasticity of Mesenchymal Stromal Cells, Stem Cell Reports, 2017.
[30] C.A. Gregory, W.G. Gunn, A. Peister, D.J. Prockop, An Alizarin red-based assay of mineralization by adherent cells in culture: comparison with cetylpyridinium chloride extraction, Anal. Biochem. 329 (1) (2004) 77–84.
[31] A.B. Nair, S. Jacob, A simple practice guide for dose conversion between animals and human, J. Basic Clin. Pharm. 7 (2) (2016) 27–31.
[32] F. Braun, M.M. Rinschen, V. Bartels, P. Frommolt, B. Habermann, J. H. Hoeijmakers, B. Schumacher, M.E. Dolle, R.U. Muller, T. Benzing, B. Schermer, C.E. Kurschat, Altered lipid metabolism in the aging kidney identified by three layered omic analysis, Aging (N Y) 8 (3) (2016) 441–457.
[33] N.W. Tietz, D.F. Shuey, D.R. Wekstein, Laboratory values in fit aging individuals-sexagenarians through centenarians, Clin. Chem. 38 (6) (1992) 1167–1185.
[34] H. Zhou, M.S. Cooper, M.J. Seibel, Endogenous glucocorticoids and bone, Bone Res 1 (2) (2013) 107–119.
[35] R.S. Weinstein, C. Wan, Q. Liu, Y. Wang, M. Almeida, C.A. O'Brien, J. Thostenson, P.K. Roberson, A.L. Boskey, T.L. Clemens, S.C. Manolagas, Endogenous glucocorticoids decrease skeletal angiogenesis, vascularity, hydration, and strength in aged mice, Aging Cell 9 (2) (2010) 147–161.
[36] C.M. Weaver, C.M. Gordon, K.F. Janz, H.J. Kalkwarf, J.M. Lappe, R. Lewis, M. O'Karma, T.C. Wallace, B.S. Zemel, The National Osteoporosis Foundation's position statement on peak bone mass development and lifestyle factors: a systematic review and implementation recommendations, Osteoporos. Int. 27 (4) (2016) 1281–1386.
[37] S. Dutta, P. Sengupta, Men and mice: relating their ages, Life Sci. 152 (2016) 244–248.
[38] J.G. Fox, The Mouse in Biomedical Research, second ed., Elsevier, AP, Amsterdam ; Boston, 2007.
[39] G.S. Baht, D. Silkstone, L. Vi, P. Nadesan, Y. Amani, H. Whetstone, Q. Wei, B. A. Alman, Exposure to a youthful circulaton rejuvenates bone repair through modulation of beta-catenin, Nat. Commun. 6 (2015) 7131.
[40] D. Nih, Consensus development panel on osteoporosis prevention, therapy, osteoporosis prevention, diagnosis, and therapy, Jama 285 (6) (2001) 785–795.
[41] R. Zhang, L. Xu, D. Zhang, B. Hu, Q. Luo, D. Han, J. Li, C. Shen, Cardioprotection of ginkgolide B on myocardial ischemia/reperfusion-induced inflammatory injury via regulation of A20-NF-kappaB pathway, Front. Immunol. 9 (2018) 2844.
[42] Z. Feng, X. Yang, L. Zhang, I.A. Ansari, M.S. Khan, S. Han, Y. Feng, Ginkgolide B ameliorates oxidized low-density lipoprotein-induced endothelial dysfunction via modulating Lectin-like ox-LDL-receptor-1 and NADPH oxidase 4 expression and inflammatory cascades, Phytother Res. 32 (12) (2018) 2417–2427.
[43] Y. Wang, Z. Gao, Y. Zhang, S.Q. Feng, Y. Liu, L.B.E. Shields, Y.Z. Zhao, Q. Zhu, D. Gozal, C.B. Shields, J. Cai, Attenuated reactive gliosis and enhanced functional recovery following spinal cord injury in null mutant mice of platelet-activating factor receptor, Mol. Neurobiol. 53 (5) (2016) 3448–3461.
[44] F. Wan, S. Zang, G. Yu, H. Xiao, J. Wang, J. Tang, Ginkgolide B suppresses methamphetamine-induced microglial activation through TLR4-NF-kappaB signaling pathway in BV2 cells, Neurochem. Res. 42 (10) (2017) 2881–2891.
[45] K. Chen, W. Sun, Y. Jiang, B. Chen, Y. Zhao, J. Sun, H. Gong, R. Qi, Ginkgolide B suppresses TLR4-mediated inflammatory response by inhibiting the phosphorylation of JAK2/STAT3 and p38 MAPK in high glucose-treated HUVECs, Oxid Med Cell Longev 2017 (2017) 9371602.
[46] Z.M. Shu, X.D. Shu, H.Q. Li, Y. Sun, H. Shan, X.Y. Sun, R.H. Du, M. Lu, M. Xiao, J. H. Ding, G. Hu, Ginkgolide B protects against ischemic stroke via modulating microglia polarization in mice, CNS Neurosci. Ther. 22 (9) (2016) 729–739.
[47] W. Chen, X. Chen, A.C. Chen, Q. Shi, G. Pan, M. Pei, H. Yang, T. Liu, F. He, Melatonin restores the osteoporosis-impaired osteogenic potential of bone marrow mesenchymal stem cells by preserving SIRT1-mediated intracellular antioxidant properties, Free Radic. Biol. Med. 146 (2020) 92–106.
[48] D. Han, X. Gu, J. Gao, Z. Wang, G. Liu, H.W. Barkema, B. Han, Chlorogenic acid promotes the Nrf2/HO-1 anti-oxidative pathway by activating p21(Waf1/Cip1) to resist dexamethasone-induced apoptosis in osteoblastic cells, Free Radic. Biol. Med. 137 (2019) 1–12.
[49] J. Gao, Z. Feng, X. Wang, M. Zeng, J. Liu, S. Han, J. Xu, L. Chen, K. Cao, J. Long, Z. Li, W. Shen, J. Liu, SIRT3/SOD2 maintains osteoblast differentiation and bone formation by regulating mitochondrial stress, Cell Death Differ. 25 (2) (2018) 229–240.
[50] S.M. Bartell, H.N. Kim, E. Ambrogini, L. Han, S. Iyer, S. Serra Ucer, P. Rabinovitch, R.L. Jilka, R.S. Weinstein, H. Zhao, C.A. O'Brien, S.C. Manolagas, M. Almeida, FoxO proteins restrain osteoclastogenesis and bone resorption by attenuating H2O2 accumulation, Nat. Commun. 5 (2014) 3773.
[51] N.K. Lee, Y.G. Choi, J.Y. Baik, S.Y. Han, D.W. Jeong, Y.S. Bae, N. Kim, S.Y. Lee, A crucial role for reactive oxygen species in RANKL-induced osteoclast differentiation, Blood 106 (3) (2005) 852–859.
[52] C. Franceschi, J. Campisi, Chronic inflammation (inflammaging) and its potential contribution to age-associated diseases, J Gerontol A Biol Sci Med Sci 69 (Suppl 1) (2014) S4–S9.
[53] T. Finkel, N.J. Holbrook, Oxidants, Oxidative stress and the biology of ageing, Nature 408 (6809) (2000) 239–247.